

## High Yield, Large Scale Synthesis of Thiolate-Protected Ag<sub>7</sub> Clusters

Zhikun Wu, Eric Lanni, Wenqian Chen, Mark E. Bier, Danith Ly, and Rongchao Jin\*

Carnegie Mellon University, Department of Chemistry, 4400 Fifth Avenue, Pittsburgh, Pennsylvania 15213

Received September 8, 2009; E-mail: rongchao@andrew.cmu.edu

Noble metal clusters have stimulated major research interest in recent years. Scientific interest in these clusters is due to their unique material properties that bridge the gap between those of small molecules (e.g., organometallic compounds) and of nanocrystals (typically >2 nm).<sup>1–4</sup> Such nanoclusters hold potential in a wide range of applications including nanoelectronics, optics, sensing, biomedicine, and catalysis.<sup>4–8</sup> For both fundamental studies and practical applications of this new type of material, the first major task is to develop synthetic methods (especially wet chemical approaches) that permit the synthesis of robust, atomically monodisperse clusters with precise control over the number of metal atoms in the cluster.

A well-established route to prepare solution phase metal clusters is to use strong ligands (such as thiols) to protect clusters and effect size control.<sup>9–12</sup> Among the noble metals, gold clusters are being extensively studied due to their chemical stability and relative ease of preparation (e.g., under ambient conditions). Some well-defined monodisperse Au<sub>n</sub> nanoclusters have been reported, and their exact formulas have been determined by mass spectrometry analysis.<sup>9–12</sup> Bimetal Au/Ag clusters, phosphine, or iron–carbonyl protected Au<sub>n</sub> clusters have also been reported.<sup>13,14</sup> Small Ag<sub>n</sub> clusters (*n* < 10 atoms) stabilized by DNA have received particular attention due to their strong fluorescence.<sup>15,16</sup> For thiolate-capped Ag clusters, no truly monodisperse Ag<sub>n</sub>(SR)<sub>m</sub> clusters have been reported. Nevertheless, there have been several notable recent studies of Ag<sub>n</sub> thiolate clusters (*n* > 10 atoms) and of chiroptical (e.g., circular dichroism) properties.<sup>17–21</sup> Very recently, Cathcart et al. reported an interesting cyclic reduction in an oxidative condition (CTOC) method to prepare silver nanoclusters; a well-defined optical spectrum was obtained for the as-prepared silver cluster.<sup>19</sup> Bakr et al. synthesized a silver thiolate species with eight absorption bands.<sup>20</sup> In another study, a 7 kDa silver cluster species was reported.<sup>21</sup> But the exact composition of these silver clusters was not attained in MS analysis,<sup>19,20</sup> although the clusters were estimated to be ~25 silver atoms. Overall, the synthesis, isolation, and precise composition determination still remain a big challenge in Ag cluster research.

Herein we report a rationally designed wet chemical method for synthesizing monodisperse Ag<sub>7</sub> clusters stabilized by four meso 2,3-dimercaptosuccinic acid (DMSA) ligands (denoted as Ag<sub>7</sub>(DMSA)<sub>4</sub>). This is the first report that achieves a precise MS determination of the composition of silver thiolate clusters. The DMSA ligand was found to be important for the synthesis of relatively stable silver clusters.

In a typical experiment (details in the Supporting Information), silver salt (AgNO<sub>3</sub>, 34.0 mg) was dissolved in ethanol (Figure 1). The solution was cooled to ~0 °C in an ice bath; DMSA was then added. After the formation of Ag<sub>x</sub>(DMSA)<sub>y</sub> intermediates, NaBH<sub>4</sub> (powders) was slowly added to the solution under vigorous stirring. The reaction mixture slowly turned from yellowish green to deep brown, indicating the reduction of Ag<sub>x</sub>(DMSA)<sub>y</sub> and formation of Ag clusters (Figure 1).

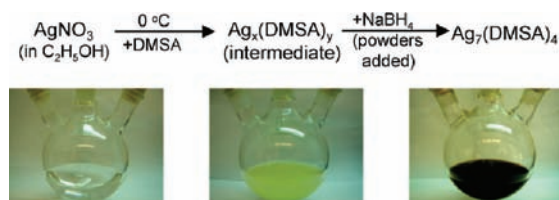


**Figure 1.** Color change during the synthesis of silver clusters. (Left) ethanol solution of AgNO<sub>3</sub>. (Middle) 4 h after addition of DMSA. (Right) 12 h after addition of NaBH<sub>4</sub>.

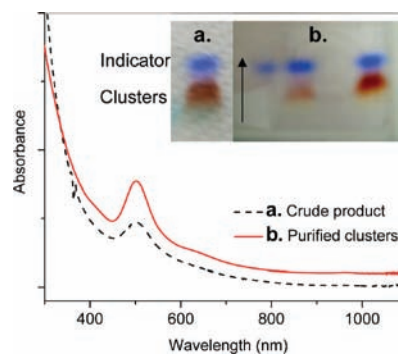


**Figure 2.** UV–vis spectra of the Ag clusters before and after purification. Inset: PAGE analysis of the (a) crude Ag clusters and (b) pure clusters after recrystallization (photograph b shows increasing loading amount of Ag clusters from left to right). Note that the blue band is from the indicator dye in the loading buffer. The arrow shows the migration direction.

The silver clusters have a low solubility in the chosen reaction medium (ethanol); hence, they spontaneously precipitated out of solution. After reaction for ~12 h, the product suspension was centrifuged briefly, and the resultant black precipitates were collected, washed thoroughly with methanol, and then dissolved in water. The aqueous solution of the as-prepared Ag clusters showed a pronounced absorption peak at ~500 nm, Figure 2 (dashed profile). To further improve the purity of the product, the clusters were precipitated by addition of MeOH. Recrystallization 2–3 times leads to highly pure Ag<sub>n</sub>(DMSA)<sub>m</sub> clusters. This purification process was evaluated by polyacrylamide gel electrophoresis (PAGE) analysis. The crude product (prior to recrystallization) shows at least two diffuse and broad bands, indicating the existence of impurities (Figure 2, inset a), while the recrystallized clusters show a more well-defined band (Figure 2, inset b), indicating a higher purity. The as-purified Ag clusters show a strong absorption peak at ~500 nm and weak peaks at ~415 and ~625 nm (Figure 2, red profile).

In our synthetic approach, DMSA was found to be an effective ligand for stabilization of silver clusters. We found that monothiols such as phenylethylthiol or dodecanethiol cannot sufficiently stabilize Ag nanoclusters, albeit these ligands have been extensively used in making gold nanoclusters.<sup>9–12,22</sup> As to the choice of reaction medium, ethanol was found to be a good medium for the

production of uniform Ag clusters. In our system, ethanol plays two important roles: (1) it acts as a size-selecting solvent by terminating or retarding the growth of clusters into larger ones since larger clusters would be less soluble in ethanol and precipitate out of solution; this provides an effective way of controlling cluster size. (2) Ethanol also acts as a reactant, and its slow reaction with  $\text{NaBH}_4$  (in the absence of water) is helpful in slowing the  $\text{Ag}_x(\text{DMSA})_y$  reduction rate and, hence, producing small and uniform Ag clusters; otherwise, if water is present, a large amount of  $\text{Ag}(0)$  species would be *instantly* produced from a rapid, uncontrolled reduction of  $\text{Ag}_x(\text{DMSA})_y$ , and the growth of Ag nuclei into clusters would be too fast and one would lose control of the cluster growth kinetics. Using the above strategy, we obtained highly monodisperse Ag nanoclusters (yield  $\sim 20\%$ ); further optimization of the reaction conditions may improve the yield. The reaction can be readily scaled up; we have tested a 6X scale-up and obtained similar yields (see Supporting Information).

To rule out the possibility that the absorption peak might arise from large Ag nanospheres (which would be  $>80$  nm diameter for a surface plasmon band at  $\sim 500$  nm) or anisotropic silver particles such as nanoprisms (which would be at least a 30 nm edge length),<sup>23</sup> we performed a high-speed centrifugation test: Ag clusters were first dissolved in water (10 mg/mL), and the solution was then centrifuged at 14 000 rpm for 30 min, but no precipitates were observed, indicating that the prepared Ag species is small clusters rather than large nanocrystals. The high electrophoretic mobility of the Ag clusters (Figure 2 inset) also implies small clusters. Moreover, TEM also confirms that the Ag particles are indeed subnanometer clusters, and no large nanocrystals were found (see Figure S1). Note that a diluted solution was used to prepare the TEM specimen to avoid cluster aggregation in TEM imaging (we observed that densely distributed Ag clusters quickly agglomerate upon electron beam irradiation under TEM). The Ag clusters are barely observable due to their extremely small size (subnanometer). Taken together, the results from high-speed centrifugation tests, electrophoresis, and TEM confirm that the Ag species synthesized in this work is composed of small clusters, and the observed optical absorption indeed originates from the clusters rather than from larger nanocrystals.

To determine the exact size of clusters (i.e., the number of Ag atoms and ligands in the cluster) is a challenging task, particularly for silver (as opposed to gold), because the isotopic distributions of silver clusters are complicated significantly by the two abundant naturally occurring silver isotopes,  $^{107}\text{Ag}$  and  $^{109}\text{Ag}$ , in addition to carbon and sulfur isotopes. In this work we have succeeded in ESI-MS analysis of intact silver clusters; this is indeed the first reported ESI-MS determination of silver thiolate clusters to our knowledge. In the ESI-MS spectrum (acquired in the negative ion mode, Figure 3A), the base peak was found at  $m/z$  1520.40 (labeled **3**, see Figure 3A inset) as a member of one isotope cluster amidst a series of similar, less-intense clusters spaced regularly to either side (labeled **1–6**). The unity spacing of the isotopes (Figure 3B) implies that the ionized clusters bear a  $-1$  charge ( $z$ ); the  $m/z$  values of the peaks therefore represent true molecule ion mass, which for the base peak of 1520.40 matches very well with the theoretical exact mass of  $[\text{Ag}_7\text{L}_4 - 2\text{H} + 2\text{Na}]^-$  (theoretical molecular weight: 1520.12, deviation 0.28), where  $\text{L} = \text{S}_2\text{C}_4\text{H}_4\text{O}_4$ , FW: 179.95). This assignment is also supported by the excellent match of the simulated and experimental isotopic distributions (Figure 3B and C). The other ions surrounding peak **3** (Figure 3A inset) correspond to the following ions:  $\text{Ag}_7\text{L}_4^-$  (1476.5, labeled **1**),  $[\text{Ag}_7\text{L}_4 - \text{H} + \text{Na}]^-$  (1498.4, labeled **2**),  $[\text{Ag}_7\text{L}_4 - 3\text{H} + 3\text{Na}]^-$  (1524.4, labeled **4**),  $[\text{Ag}_7\text{L}_4 - 4\text{H} + 4\text{Na}]^-$  (1564.4, labeled **5**),  $[\text{Ag}_7\text{L}_4 - 5\text{H} + 5\text{Na}]^-$

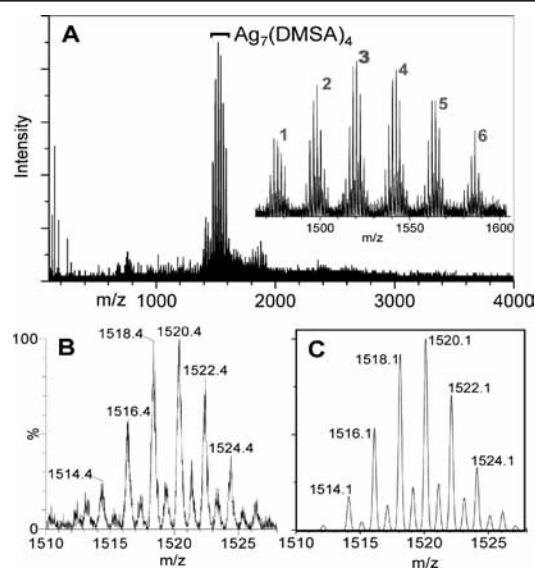


**Figure 3.** (A) ESI spectra of silver clusters (negative ion mode, inset shows the zoomed-in spectrum). (B) and (C) show the experimental and simulated isotopic pattern of  $\text{Ag}_7\text{L}_4 - 2\text{H} + 2\text{Na}$ , respectively.

(1586.4, labeled **6**). The assignments are supported by their isotopic distribution patterns (see Figure S2) as well as the 22 Da spacing ( $22 = m_{\text{Na}} - m_{\text{H}}$ ).

On the basis of the assigned peaks as well as the negative ion nature, we conclude that the native cluster is composed of 7 silver atoms stabilized by 4 DMSA ligands and the  $\text{Ag}_7$  core carries a  $-1$  charge. The emergence of a series of H subtraction/Na addition ( $-\text{H} + \text{Na}$ ) peaks does not affect the cluster's original charge.

We have also performed matrix-assisted laser desorption ionization (MALDI) MS analysis (matrix: sinapic acid). Compared to ESI-MS, MALDI forms and detects ions over a much higher  $m/z$  range yet fragmentation is often observed. For the  $\text{Ag}_7(\text{DMSA})_4$  clusters, a set of peaks centered at  $\sim 1500$   $m/z$  (singly charged, assigned to  $\text{Ag}_7\text{L}_4 - \text{H} + \text{Na}$ ) with a spacing of 22 (i.e.,  $m_{\text{Na}} - m_{\text{H}}$ ) were found in MALDI-MS analysis (Figure S3), which is consistent with the ESI results. The other sets of peaks at lower  $m/z$  values are fragments resulted from the  $\text{Ag}_7\text{L}_4$  ions since they were not found in ESI analysis. No larger  $\text{Ag}_n$  clusters were found in the high mass range (up to  $m/z$  20 000), confirming the monodispersity of the prepared  $\text{Ag}_7(\text{DMSA})_4$  clusters.

The MS/MS experiments also confirmed that the cluster is composed of 7 silver atoms. In MS/MS analysis, the dianion  $[\text{Ag}_7\text{L}_4 - 3\text{H} + 2\text{Na}]^{2-}$  ( $m/z$  759.57) was chosen as the parent ion. The ion was subject to further collision at different energies, and the fragmentation pattern was analyzed. When the collision voltage was set at 10 V, the parent ion loses a neutral fragment ( $\text{SC}_4\text{O}_4\text{H}_4$ ,  $73.99 \times 2 = 147.98$  Da,  $\text{SC}_4\text{O}_4\text{H}_3$  observed at  $m/z = 146.99$ ) of one of the four ligands but a sulfur atom of the ligand is still retained on the cluster due to Ag–S bonding, forming  $\text{Ag}_7\text{S}(\text{S}_2\text{C}_4\text{O}_4\text{H}_4)(\text{S}_2\text{C}_4\text{O}_4\text{H}_3\text{Na})(\text{S}_2\text{C}_4\text{O}_4\text{H}_2\text{Na})$  ( $m/z$  685.57,  $z = -2$ ; note that the  $\text{Ag}_7$  core bears a  $-1$  charge and the other negative charge arises from one ligand bearing  $\text{COO}^-$ ), Figure 4A. At 25–40 V, the rest of the ligands break up but one S atom from each ligand is retained on the cluster, forming fragments ( $\text{Ag}_7\text{S}_4^-$ ), Figure 4B. Apparently the negative charge on the  $\text{Ag}_7$  core is retained, consistent with the ESI assignment of  $\text{Ag}_7\text{L}_4^-$ . With increasing voltage, smaller fragments were sequentially observed, including  $\text{Ag}_6\text{S}_4^-$  and  $\text{Ag}_5\text{S}_4^-$  (Figure 4C–D).

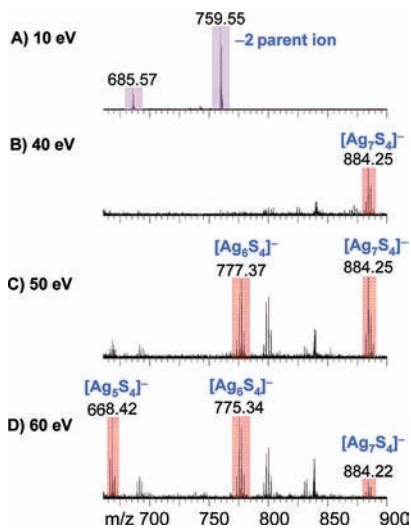


**Figure 4.** MS/MS analysis of the clusters (dianion  $[\text{Ag}_7\text{L}_4 - 3\text{H} + 2\text{Na}]^{2-}$ ).

The observation of  $[\text{Ag}_7\text{S}_4]^{2-}$  in the MS/MS experiment may indicate that only one thiol group in the DMSA ligand binds to the  $\text{Ag}_7$  core, while the other thiol group perhaps form a S–S bond with a neighboring ligand. It is meaningful to count the number of valence electrons in the cluster, i.e.,  $7 - 4 + 1 = 4e$  (assuming each thiolate ligand consumes one electron due to Ag–S bond formation). The presence of 4 valence electrons should explain the observed distinct optical absorption band at  $\sim 500$  nm (see Figure 2). This explanation is also supported by our previous observation of an optical absorption at  $\sim 485$  nm in  $\text{Au}_{20}(\text{SR})_{16}$  clusters, in which the number of valence electrons is  $20 - 16 = 4$ .<sup>12a</sup> For the  $\text{Au}_{20}(\text{SR})_{16}$  cluster, DFT calculations have predicted a  $\text{Au}_8$  core capped by 4  $\text{RS}(\text{AuSR})_3$  motifs.<sup>24</sup>

An interesting question pertains to the atomic packing structure that might be adopted in the  $\text{Ag}_7(\text{DMSA})_4$  cluster. Since the four DMSA ligands have eight thiol groups, apparently not all the thiol groups bind to the  $\text{Ag}_7$  core; otherwise the cluster would be a  $\text{Ag}(\text{I})$  complex, which has no color.<sup>25</sup> Previously, DFT calculations on the 3D and planar isomers of bare  $\text{Au}_7$  clusters have been reported.<sup>26</sup> The bare anionic  $\text{Au}_7^-$  seems to favor a planar structure,<sup>27a</sup> while  $\text{Ag}_7$  clusters favor a pentagonal bipyramidal structure.<sup>27b</sup> Since bare clusters and ligand-protected ones have fundamental differences in many aspects, the structures of bare  $\text{Au}_7$  may not apply to  $\text{Ag}_7(\text{DMSA})_4$ . It is worth noting that an interesting heptamer cluster—a  $\text{Au}_6\text{Ag}$  wheel with a gold rim—was previously reported by Cerrada et al.<sup>28</sup> In the case of  $\text{Au}_{25}(\text{SR})_{18}$  clusters, the cluster was composed of an icosahedral kernel ( $\text{Au}_{13}, D_{2h}$ ) wrapped by six –S–Au–S–Au–S– staples along the three mutually perpendicular 2-fold axes.<sup>3a,29</sup> The extended staple motifs seem difficult to be applied to the  $\text{Ag}_7(\text{DMSA})_4$  cluster. The exact structure of  $\text{Ag}_7(\text{DMSA})_4$  remains to be revealed by X-ray crystallography in future work.

In summary, in this work we have devised a facile synthetic route for preparing well-defined, monodisperse  $\text{Ag}_7(\text{DMSA})_4$  clusters in high yield. The cluster composition was determined by mass spectrometry. This is the first time that the exact composition of a silver thiolate cluster is fully analyzed by MS. Previous work has not attained determination of the exact composition of Ag thiolate clusters. Future work includes solving their crystal structure and correlating the structure with properties as well as size-controllable synthesis of silver nanoclusters.

**Acknowledgment.** This work is financially supported by CMU & AFOSR. We thank Dr. Joseph Suhan for TEM assistance.

**Supporting Information Available:** Experimental details of the synthesis and characterization of silver nanoclusters. This material is available free of charge via the Internet at <http://pubs.acs.org>.

## References

- (1) (a) Wyrwas, R. B.; Alvarez, M. M.; Khoury, J. T.; Price, R. C.; Schaaff, T. G.; Whetten, R. L. *Eur. Phys. J. D* **2007**, *43*, 91. (b) de Silva, N.; Dahl, L. F. *Inorg. Chem.* **2005**, *44*, 9604. (c) Ott, L. S.; Finke, R. G. *Inorg. Chem.* **2006**, *45*, 8382.
- (2) (a) Wilcoxon, J. P.; Abrams, B. L. *Chem. Soc. Rev.* **2006**, *35*, 1162. (b) Woehle, G. H.; Warner, M. G.; Hutchison, J. E. *J. Phys. Chem. B* **2002**, *106*, 9979.
- (3) (a) Zhu, M.; Aikens, C. M.; Hollander, F. J.; Schatz, G. C.; Jin, R. *J. Am. Chem. Soc.* **2008**, *130*, 5883. (b) Aikens, C. M. *J. Phys. Chem. C* **2008**, *112*, 19797.
- (4) Schmid, G. *Chem. Soc. Rev.* **2008**, *37*, 1909.
- (5) (a) Wohltjen, H.; Snow, A. W. *Anal. Chem.* **1998**, *70*, 2856. (b) Rowe, M. P.; Plass, K. E.; Kim, K.; Kurdak, C.; Zellers, E. T.; Matzger, A. J. *Chem. Mater.* **2004**, *16*, 3513.
- (6) Ackerson, C. J.; Jadzinsky, P. D.; Jensen, G. J.; Kornberg, R. D. *J. Am. Chem. Soc.* **2006**, *128*, 2635.
- (7) (a) Gu, T.; Whitesell, J. K.; Fox, M. A. *Chem. Mater.* **2003**, *15*, 1358. (b) Ramakrishna, G.; Varnavski, O.; Kim, J.; Lee, D.; Goodson, T. *J. Am. Chem. Soc.* **2008**, *130*, 5032. (c) Zhou, R. J.; Shi, M. M.; Chen, X. Q.; Wang, M.; Chen, H. Z. *Chem.—Eur. J.* **2009**, *15*, 4944.
- (8) Maye, M. M.; Luo, J.; Han, L.; Kariuki, N.; Zhong, C. *J. Gold Bull.* **2003**, *36*, 75.
- (9) (a) Schaaff, T. G.; Knight, G.; Shafiqullin, M. N.; Borkman, R. F.; Whetten, R. L. *J. Phys. Chem. B* **1998**, *102*, 10643. (b) Wang, Z.; Tan, B.; Hussain, I.; Schaeffer, N.; Wyatt, M. F.; Brust, M.; Cooper, A. I. *Langmuir* **2007**, *23*, 885.
- (10) (a) Dass, A.; Stevenson, A.; Dubay, G. R.; Tracy, J. B.; Murray, R. W. *J. Am. Chem. Soc.* **2008**, *130*, 5940. (b) Kim, J.; Lema, K.; Ukaigwe, M.; Lee, D. *Langmuir* **2007**, *23*, 7853. (c) Dass, A. *J. Am. Chem. Soc.* **2009**, *131*, 11666.
- (11) (a) Shichibu, Y.; Negishi, Y.; Tsukuda, T.; Teranishi, T. *J. Am. Chem. Soc.* **2005**, *127*, 13464. (b) Negishi, Y.; Chaki, N. K.; Shichibu, Y.; Whetten, R. L.; Tsukuda, T. *J. Am. Chem. Soc.* **2007**, *129*, 11322.
- (12) (a) Zhu, M.; Qian, H.; Jin, R. *J. Am. Chem. Soc.* **2009**, *131*, 7220. (b) Qian, H.; Zhu, M.; Andersen, U. N.; Jin, R. *J. Phys. Chem. A* **2009**, *113*, 4281.
- (13) (a) Teo, B. K.; Keating, K. *J. Am. Chem. Soc.* **1984**, *106*, 2224. (b) Schmid, G.; Boese, R.; Pfeil, R.; Bandermann, F.; Meyer, S.; Calis, G. H. M.; van der Velden, J. W. A. *Chem. Ber.* **1981**, *114*, 3634. (c) Wen, F.; Englert, U.; Guttrath, B.; Simon, U. *Eur. J. Inorg. Chem.* **2008**, 106. (d) Schulz-Dobrick, M.; Jansen, M. *Angew. Chem., Int. Ed.* **2008**, *47*, 2256.
- (14) (a) Femoni, C.; Iapalucci, M. C.; Longoni, G.; Tiozzo, C.; Zacchini, S. *Angew. Chem., Int. Ed.* **2008**, *47*, 6666. (b) Lopez-Acevedo, O.; Rintala, J.; Virtanen, S.; Femoni, C.; Tiozzo, C.; Gronbeck, H.; Pettersson, M.; Hakkinen, H. *J. Am. Chem. Soc.* **2009**, *131*, 12573.
- (15) (a) Yu, J.; Choi, S.; Dickson, R. M. *Angew. Chem., Int. Ed.* **2009**, *48*, 318. (b) Ritchie, C. M.; Johnsen, K. R.; Kiser, J. R.; Antoku, Y.; Dickson, R. M.; Petty, J. T. *J. Phys. Chem. C* **2007**, *111*, 175.
- (16) Dlez, I.; Pusa, M.; Kulmala, S.; Jiang, H.; Walther, A.; Goldmann, A. S.; Müller, A. H. E.; Ikkala, O.; Ras, R. H. A. *Angew. Chem., Int. Ed.* **2009**, *48*, 2122.
- (17) Branham, M. R.; Douglas, A. D.; Mills, A. J.; Tracy, J. B.; White, P. S.; Murray, R. W. *Langmuir* **2006**, *22*, 11376.
- (18) Nishida, N.; Yao, H.; Kimura, K. *Langmuir* **2008**, *24*, 2759.
- (19) Cathcart, N.; Mistry, P.; Makra, C.; Pietrobon, B.; Coombs, N.; Jelokhani-Niaraki, M.; Kitaev, V. *Langmuir* **2009**, *25*, 5840.
- (20) Bakr, O. M.; Amendola, V.; Aikens, C. M.; Wenselers, W.; Li, R.; Negro, L. D.; Schatz, G. C.; Stellacci, F. *Angew. Chem., Int. Ed.* **2009**, *48*, 1.
- (21) Mrudula, K. V.; Rao, T. U. B.; Pradeep, T. *J. Mater. Chem.* **2009**, *19*, 4335.
- (22) (a) Wu, Z.; Suhan, J.; Jin, R. *J. Mater. Chem.* **2009**, *19*, 622. (b) Wu, Z.; Gayathri, C.; Gil, R.; Jin, R. *J. Am. Chem. Soc.* **2009**, *131*, 6535. (c) Wu, Z.; Jin, R. *ACS Nano* **2009**, *3*, 2036.
- (23) Jin, R.; Cao, Y. W.; Hao, E.; Metraux, G. S.; Schatz, G. C.; Mirkin, C. A. *Nature* **2003**, *425*, 487.
- (24) (a) Pei, Y.; Gao, Y.; Shao, N.; Zeng, X. C. *J. Am. Chem. Soc.* **2009**, *131*, 13619. (b) Jiang, D.-e.; Chen, W.; Whetten, R. L.; Chen, Z. *J. Phys. Chem. C* **2009**, *113*, 16983.
- (25) Dance, I.; Fisher, K. *Prog. Inorg. Chem.* **1994**, *41*, 637–803.
- (26) Tian, W. Q.; Ge, M.; Sahu, B. R.; Wang, D.; Yamada, T.; Mashiko, S. *J. Phys. Chem. A* **2004**, *108*, 3806.
- (27) (a) Hakkinen, H.; Moseler, M.; Landman, U. *Phys. Rev. Lett.* **2002**, *89*, 033401. (b) Lee, H. M.; Ge, M.; Sahu, B. R.; Tarakeshwar, P.; Kim, K. S. *J. Phys. Chem. B* **2003**, *107*, 9994.
- (28) Cerrada, E.; Contel, M.; Valencia, A. D.; Laguna, M.; Gelbrich, T.; Hursthouse, M. B. *Angew. Chem., Int. Ed.* **2000**, *39*, 2353.
- (29) Zhu, M.; Eckenhoff, W. T.; Pintauer, T.; Jin, R. *J. Phys. Chem. C* **2008**, *112*, 14221.

JA907627F